Alternative solvable description of the E(5) critical point symmetry in the interacting boson model

Feng Pan, Yu Zhang, Hao-Cheng Xu, Lian-Rong Dai, and J. P. Draayer

Phys. Rev. C **91**, 034305 — Published 3 March 2015

DOI: 10.1103/PhysRevC.91.034305

An Alternative Solvable Description of the E(5) Critical Point Symmetry in the Interacting Boson Model

Feng Pan,[1,2] Yu Zhang,[1] Hao-Cheng Xu,[1] Lian-Rong Dai,[1] and J. P. Draayer[2]

[1]*Department of Physics, Liaoning Normal University, Dalian 116029, P. R. China*
[2]*Department of Physics and Astronomy, Louisiana State University, Baton Rouge, Louisiana 70803-4001, USA*

(Dated: February 18, 2015)

A solvable extended Hamiltonian that includes multi-pair interactions among s- and d-bosons up to infinite order within the framework of the interacting boson model is proposed to gain a better description of E(5) model results for finite-N systems. Numerical fits to low-lying energy levels and reduced E2 transition rates within this extended version of the theory are presented for various N values. It shows that the extended Hamiltonian within the IBM provides a better description of the E(5) model results for small N cases, while the results of the model in the large-N cases are close to those of the E(5)-β^{2n} type models studied previously.

PACS numbers: 21.60.Fw, 21.60.Ev, 21.10.Re

I. Introduction

Quantum phase transitions signal important phenomena in various quantum many-body systems [1]. In atomic nuclei, the quantum phase transitions are often related to different geometrical shapes of the system, which can be described either by the Bohr-Mottelson model (BMM) [2] or by the Interacting Boson Model (IBM) [3]. Generally, in either the BMM or the IBM, a Hamiltonian that is suitable to describe such (shape) phase transitions can be solved numerically. However, with suitable simplification, Iachello proposed an exactly solvable model [4] within the BMM, which is called the E(5) (critical point symmetry) model suitable to describe the critical phenomena in the vibration to γ-unstable (shape) phase transition. The potential used in the E(5) model only depends on the β degree of freedom with an infinite square well. It has been shown that there are many nuclei with the E(5) critical point symmetry, such as ^{134}Ba [5], ^{104}Ru [6], ^{102}Pd [7], ^{108}Pd [8], and ^{116}Cd [9]. Inspired by the E(5) model, Lévai and Arias studied the Bohr Hamiltonian with a sextic potential and a centrifugal barrier, of which quasi-exact solutions can be derived [10], while Bonatsos *et al* explored numerical solutions for the γ-independent Bohr Hamiltonian with β^{2n} potentials for $n \geq 1$ called the confined γ-soft rotor model [11], in which the spectra and transition rates for the β^{2n} potentials for $2 \leq n \leq 4$ are given explicitly and compared with the original E(5) model.

Since the E(5) model is simple and suitable to describe the critical point symmetry of the vibration to γ-unstable (shape) phase transition in the BMM, it is interesting to seek a suitable Hamiltonian near the critical point of the $U(5)$-$O(6)$ transitional region to describe this critical point symmetry because the vibration to γ-unstable (shape) phase transition is equivalently describable in the IBM along the integrable line from U(5) to O(6) [3, 12]. Arias *et al* did initial work along this line [13, 14], showing that for the low-lying part of the spectrum the results of the consistent-Q type $U(5)$-$O(6)$ Hamiltonian in the IBM at the critical point are close to those of the E(5) model for cases with a small number of bosons, while the IBM Hamiltonian for large N cases reproduces low-lying parts of the spectrum and electromagnetic transition rates of a BMM Hamiltonian with a β^4 potential. A detailed study on the connections between the E(5), E(5)-β^4, E(5)-β^6, and E(5)-β^8 models based on particular solutions of the BMM with such γ-unstable potentials and the IBM fit with relatively large N $(= 60)$ were also carried out [15], which further confirms the above conclusions.

As is well known, the number of bosons in the IBM is phenomenologically regarded as the number of valence nucleon pairs. In realistic nuclear systems, the number of bosons is always finite. It is expected that a suitable IBM Hamiltonian, like the U(5), O(6), and SU(3) limiting cases, may fit the E(5) critical point nuclei better, especially when relatively higher excited levels are taken into consideration, though it is commonly believed that the BMM may be regarded as the large-N limit of the IBM [16–18]. The purpose of this work is to establish an extended Hamiltonian near the critical point of the $U(5)$-$O(6)$ transitional region of the IBM, of which the solution should be closer to that of the E(5) model with finite N. Namely, the model is suitable to describe the E(5) critical symmetry nuclei as reported in [5–9], while the model in the large-N cases may be close to those of the E(5)-β^{2n} type models similar to the results reported in [15].

II. A solvable Hamiltonian near the $U(5)$-$O(6)$ critical point

Similar to the well-known consistent-Q formalism in the IBM [3, 13, 14], using up to two-body interactions the $U(5)$-$O(6)$ Hamiltonian may be schematically written as [12–14, 19]

$$\hat{H} = g\left(x\hat{n}_d + \frac{1-x}{N}\hat{P}^\dagger\hat{P}\right), \tag{1}$$

where g is a real parameter, the control parameter $x \in [0,1]$, $\hat{n}_d = \sum_\mu d^\dagger_\mu d_\mu$ is the d-boson number operator, and

$$P^\dagger = \frac{1}{2}(d^\dagger \cdot d^\dagger - s^{\dagger 2}) \tag{2}$$

is the boson pairing operator. As shown in [13, 14], the spectrum and E2 transition rates generated from (1) at the critical point with $x \sim 1/2$ approach those of the Bohr Hamiltonian with a β^4 potential rather than to those of the E(5) model in the large-N limit.

In order to clarify the structure of the $U(5)$-$O(6)$ transitional solutions, similar to [12–14], we introduce the s- and d-boson SU(1,1) pairing algebras with

$$S_d^+ = (S_d^-)^\dagger = \frac{1}{2} d^\dagger \cdot d^\dagger,\ S_d^0 = \frac{1}{2}\hat{n}_d + \frac{5}{4}, \tag{3}$$

$$S_s^+ = (S_s^-)^\dagger = \frac{1}{2} s^{\dagger 2},\ S_s^0 = \frac{1}{2}\hat{n}_s + \frac{1}{4}, \tag{4}$$

where $\hat{n}_s$ are the number operator for s-bosons, which satisfy the following commutation relations:

$$[S_\sigma^+, S_\rho^-] = -2\delta_{\sigma\rho} S_s^0,\ \ [S_\sigma^0, S_\rho^\pm] = \pm\delta_{\sigma\rho} S_\rho^\pm. \tag{5}$$

The Casimir operator of $\mathrm{SU}_\rho(1,1)$ can be expressed as

$$C_2(\mathrm{SU}_\rho(1,1)) = \mathrm{S}_\rho^0(\mathrm{S}_\rho^0 - 1) - \mathrm{S}_\rho^+\mathrm{S}_\rho^-, \tag{6}$$

in which the Casimir operator of $\mathrm{SU}_d(1,1)$ is related to the Casimir operator of O(5) with

$$C_2(\mathrm{SU}_d(1,1)) = \frac{1}{4}\mathrm{C}_2(\mathrm{O}(5)) + \frac{5}{16}. \tag{7}$$

Thus, the pairing operators appearing in (1) can be regarded as the results of the SU(1,1) coupling:

$$P^\dagger = S_d^+ - S_s^+,\ P = S_d^- - S_s^-, \tag{8}$$

which, together with

$$P^0 = S_d^0 + S_s^0, \tag{9}$$

generate $\mathrm{SU}_{sd}(1,1)$ algebra. The Casimir operator of $\mathrm{SU}_{sd}(1,1)$ is related to the Casimir operator of O(6) with

$$C_2(\mathrm{SU}_{sd}(1,1)) = P^0(P^0-1) - P^\dagger P = \frac{1}{4}C_2(\mathrm{O}(6)) + \frac{3}{4}. \tag{10}$$

Under the $U(6) \supset U(5) \supset O(5) \supset O(3)$ basis, the generators of either $SU_d(1,1)$ or $SU_s(1,1)$ commute with all generators of $O(5)$. Therefore, the basis vectors of $U(6) \supset U(5) \supset O(5) \supset O(3)$ are simultaneously the basis vectors of $SU_d(1,1)$. Let $|\kappa\nu\rangle$ be basis vectors of an irreducible representation (irrep) of SU(1,1), where κ can be any positive real number, and $\nu = \kappa,\ \kappa+1, \cdots$. We have

$$C_2(\mathrm{SU}(1,1))|\kappa\nu\rangle = \kappa(\kappa-1)|\kappa\nu\rangle, S^0|\kappa\nu\rangle = \nu|\kappa\nu\rangle. \tag{11}$$

The complementary relation between the basis vectors of $U(6) \supset U(5) \supset O(5) \supset O(3)$ and those of $\mathrm{SU}_d(1,1)\otimes\mathrm{SU}_s(1,1)$ can be expressed as

$$\begin{aligned} |Nn_d\tau\alpha LM\rangle = |\kappa_d = \tfrac{\tau}{2} + \tfrac{5}{4}, \nu_d = \tfrac{n_d}{2} + \tfrac{5}{4}; \\ \kappa_s = \tfrac{\tau_s}{2} + \tfrac{1}{4}, \nu_s = \tfrac{n_s}{2} + \tfrac{1}{4}; \alpha LM\rangle, \end{aligned} \tag{12}$$

where N is the total number of bosons, n_d is the number of d-bosons, τ is the seniority quantum number labeling the irrep of $O(5)$, L is the angular momentum quantum number of $O(3)$, α is an additional quantum number needed to distinguish different states with the same L, M is the quantum number of the third component of the angular momentum, $\tau_s = 0$ or 1 according to $N-\tau$ is even or odd, and $n_s = N - n_d$ is the number of s-bosons. Therefore, for given N, τ, α, L, and M, the orthonormalized basis vectors of $U(6) \supset U(5) \supset O(5) \supset O(3)$ can be equivalently expressed as those of $\mathrm{SU}_d(1,1)\otimes\mathrm{SU}_s(1,1)$ with

$$\begin{aligned} |\xi\rangle \equiv |\tau_s; \xi; \tau\alpha LM\rangle = \\ \mathscr{N}(S_s^+)^{\frac{N-\tau-\tau_s}{2}-\xi}(S_d^+)^\xi |\tau_s; \tau\alpha LM\rangle, \end{aligned} \tag{13}$$

of which $n_d = 2\xi + \tau$, where the normalization constant

$$\mathscr{N} = \left(\frac{2^{N-\tau-\tau_s-2\xi}(2\tau+3)!!}{\xi!(N-\tau-2\xi)!(2\tau+2\xi+3)!!} \right)^{\frac{1}{2}}, \tag{14}$$

and $\xi = 0, 1, 2, \cdots, \frac{1}{2}(N-\tau-\tau_s)$. The matrix representations of $SU_d(1,1)$ and $SU_s(1,1)$ under the basis vectors (13) are given by

$$\begin{aligned} S_d^+|\xi\rangle = \tfrac{1}{2}\sqrt{(2\xi+2)(2\tau+2\xi+5)}|\xi+1\rangle, \\ S_d^-|\xi\rangle = \tfrac{1}{2}\sqrt{2\xi(2\tau+2\xi+3)}|\xi-1\rangle, \\ S_d^0|\xi\rangle = \tfrac{1}{2}(\tau+2\xi+\tfrac{5}{2})|\xi\rangle, \end{aligned} \tag{15}$$

and

$$\begin{aligned} S_s^+|\xi\rangle = \tfrac{1}{2}\sqrt{(N-\tau-2\xi)(N-\tau-2\xi-1)}|\xi+1\rangle, \\ S_s^-|\xi\rangle = \tfrac{1}{2}\sqrt{(N-\tau-2\xi+2)(N-\tau-2\xi+1)}|\xi-1\rangle, \\ S_s^0|\xi\rangle = \tfrac{1}{2}(N-\tau-2\xi+\tfrac{1}{2})|\xi\rangle. \end{aligned} \tag{16}$$

Thus, $P^\dagger P$ under the basis vectors (13) is tridiagonal. The matrix elements of the diagonal part can be expressed as

$$\begin{aligned} \langle\xi|\left(S_d^+S_d^- + S_s^+S_s^-\right)|\xi\rangle = \tfrac{1}{4}(2\xi)(2\tau+2\xi+3) + \\ \tfrac{1}{4}(N-\tau-2\xi)(N-\tau-2\xi-1), \end{aligned} \tag{17}$$

while those of the nonzero non-diagonal parts are given by

$$\begin{aligned} \langle\xi+1|S_d^+S_s^-|\xi\rangle = \tfrac{1}{4}((N-\tau-2\xi)(N-\tau-2\xi-1)\times \\ (2\xi+2)(2\tau+2\xi+5))^{\frac{1}{2}}, \end{aligned} \tag{18}$$

$$\langle\xi-1|S_s^+S_d^-|\xi\rangle=\tfrac{1}{4}((N-\tau-2\xi+2)(N-\tau-2\xi+1)\times (2\xi)(2\tau+2\xi+3))^{\frac{1}{2}}. \quad (19)$$

It is clear that the U(5)-O(6) transitional phase is mainly driven by the nonzero non-diagonal part of $P^\dagger P$. The critical value of the control parameter $x_c\sim 0.5$ in this case as shown in [14, 19].

Using the $SU_d(1,1)$ and $SU_s(1,1)$ generators, we can build an extended IBM Hamiltonian (EXT) as

$$\hat{H}_c=\Delta\hat{n}_d+\tfrac{\lambda}{N}(S_s^+S_s^-+S_d^+S_d^-)- g_2\textstyle\sum_{k=1}^{\infty}(\tilde{S}_s^{+k}\tilde{S}_d^{-k}+\tilde{S}_d^{+k}\tilde{S}_s^{-k}), \quad (20)$$

where $\Delta=\varepsilon_d-\varepsilon_s>0$ is the energy gap of s- and d-bosons, $\lambda>0$ and $g_2>0$ are real parameters. Obviously, (20) becomes (1) when $g_2=\lambda/N$ and only the $k=1$ term with the replacement $\tilde{S}_\rho^\pm\to S_\rho^\pm$ is included in the third term of (20). The second term in (20) is the same as the diagonal part of the boson pairing interactions included in (1), while the third term contributes to the non-diagonal part of the boson pairing interactions but not restricted with the tridiagonal form shown by (18) and (19) when it is diagonalized within the subspace spanned by basis vectors shown in (13), in which

$$\tilde{S}_d^+=S_d^+\tfrac{1}{\sqrt{(S_d+S_d^0)(S_d^0-S_d+1)}},\ \ \tilde{S}_d^-=\left(S_d^+\right)^\dagger,$$
$$\tilde{S}_s^+=S_s^+\tfrac{1}{\sqrt{(S_s+S_s^0)(S_s^0-S_s+1)}},\ \ \tilde{S}_s^-=\left(S_s^+\right)^\dagger. \quad (21)$$

Instead of the operators $\{\tilde{S}_\rho^\pm\}$, one can also use the usual boson pairing operators $\{S_\rho^\pm\}$ to construct the multi-pair interactions similar to the third term of (20). In this case, the problem, however, is no longer exactly solvable.

It should be noted that the quantum numbers of S_d, S_d^0, and S_s, S_s^0 in (21) are κ_d, ν_d, and κ_s, ν_s, respectively, under the $U(6)\supset U(5)\supset O(5)\supset O(3)$ basis shown in (12). Therefore, the operators appearing in (21) are well-defined under the basis vectors (13). Since $\tilde{S}_d^\pm$ and $\tilde{S}_s^\pm$ are built from the original $SU_\rho(1,1)$ algebras, of which the irreducible representations (irreps) are still lower bound. For a given irrep $|\kappa\nu\rangle$ of the SU(1,1), $\tilde{S}^\pm$ behave like the unit shift operators:

$$\tilde{S}^\pm|\kappa\nu\rangle=|\kappa\nu\pm1\rangle. \quad (22)$$

Thus, in contrast to (5), the operators $\{\tilde{S}_d^+,\tilde{S}_d^-,S_d^0\}$ and $\{\tilde{S}_s^+,\tilde{S}_s^-,S_s^0\}$ under the corresponding SU(1,1) irreps satisfy the following commutation relations:

$$[\tilde{S}_\sigma^+,\tilde{S}_\rho^-]=-\delta_{\rho\sigma}\delta_{S_\rho S_\rho^0},\ \ [S_\sigma^0,\tilde{S}_\rho^\pm]=\pm\delta_{\sigma\rho}S_\rho^\pm. \quad (23)$$

Hence, $\{\tilde{S}_d^+,\tilde{S}_d^-,S_d^0\}$ and $\{\tilde{S}_s^+,\tilde{S}_s^-,S_s^0\}$ are two copies of the generators of E_2 algebra when $S_\rho^0\neq S_\rho$, which become those of the Heisenberg algebra only when $S_\rho^0=S_\rho$. They will be called as the $\tilde{E}_2$ algebra.

Similar to the consistent-Q formulism [12] in describing the U(5)-O(6) transitional nuclei, the Hamiltonian (20) is also exactly solvable. To digonalize the Hamiltonian (20), we use the simple algebraic Bethe ansatz with

$$|N,\zeta,\tau\alpha L\rangle=\sum_{\xi=0}^{\frac{1}{2}(N-\tau-\tau_s)}C_\xi^{(\zeta)}|\xi\rangle, \quad (24)$$

where $|\xi\rangle\equiv|\tau_s;\xi;\tau\alpha LM\rangle$ as given in (13), and $C_\xi^{(\zeta)}$ is the expansion coefficient to be determined. Similar to the procedures used in [20], it can be proven that the expansion coefficient $C_\xi^{(\zeta)}$ can be expressed as

$$C_\xi^{(\zeta)}=\frac{1}{F^{(\zeta)}(\xi)}, \quad (25)$$

where

$$F^{(\zeta)}(\xi)=E_{\tau,L}^{(\zeta)}-g_2-\tfrac{\lambda}{2N}\xi(2\tau+2\xi+3)- \tfrac{\lambda}{4N}(N-\tau-2\xi)(N-\tau-2\xi-1)-\Delta(\tau+2\xi), \quad (26)$$

in which $E_{\tau,L}^{(\zeta)}$ is the ζ-th eigen-energy for given τ and L. To show that (24) and (25) are indeed consistent, one may directly apply the Hamiltonian (20) on the N-particle state (24) to establish the eigen-equation $\hat{H}_c|N,\zeta\rangle=E_{\tau,L}^{(\zeta)}|N,\zeta\rangle$. After simple algebraic manipulation, one can easily find that

$$-g_2\sum_{k=1}^{\infty}(\tilde{S}_s^{+k}\tilde{S}_d^{-k}+\tilde{S}_d^{+k}\tilde{S}_s^{-k})|N,\zeta,\tau\alpha,LM\rangle=$$

$$g_2|N,\zeta,\tau\alpha,LM\rangle-g_2\sum_{\xi'}C_{\xi'}^{\xi}\sum_{\xi}|\xi\rangle. \quad (27)$$

Once the expansion coefficients are chosen as those shown in (25), the eigen-equation $\hat{H}_c|N,\zeta\rangle=E_{\tau,L}^{(\zeta)}|N,\zeta\rangle$ is fulfilled when and only when

$$-g_2\sum_{\xi}\frac{1}{F^{(\zeta)}(\xi)}=1. \quad (28)$$

Solutions of (28) provide eigenvalues $E_{\tau,L}^{(\zeta)}$ and the corresponding eigenstates (24) simultaneously.

For given N, τ, and L, let $F^{(\zeta)}(\xi)=E_{\tau,L}^{(\zeta)}-x_\xi$ according to (26). Generally, $x_0\neq x_1\neq x_2\neq\cdots\neq x_{\frac{1}{2}(N-\tau-\tau_s)}$ is always satisfied. Let $V_q(x_i)$ be exact value of x_i with the ordering $V_0<V_1<\cdots<V_{\frac{1}{2}(N-\tau-\tau_s)}$. Zeros of the polynomial related with (28), $E_{\tau,L}^{(\zeta)}$, satisfy either the interlacing condition $V_0<E_{\tau,L}^{(1)}<V_1<E_{\tau,L}^{(2)}<V_2<\cdots$ or $-\infty<E_{\tau,L}^{(1)}<V_0<$

$E^{(2)}_{\tau,L} < V_1 < \cdots$, which is very much helpful in finding roots of Eq. (28). Actually, the polynomials related with Eq. (28) is a special case of the extended Stieltjes polynomials [21]. Since $V_0, V_1, \cdots, V_{\frac{1}{2}(N-\tau-\tau_s)}$ are real and not equal one another, the zeros of the polynomials related with Eq. (28) are either within $\frac{1}{2}(N-\tau-\tau_s)+1$ open intervals $(-\infty, V_0)$, (V_1, V_2), $\cdots$, $(V_{\frac{1}{2}(N-\tau-\tau_s)-1}, V_{\frac{1}{2}(N-\tau-\tau_s)})$ or within (V_0, V_1), (V_1, V_2),$\cdots$, $(V_{\frac{1}{2}(N-\tau-\tau_s)}, +\infty)$. Binomials $F^{(\zeta)}(\xi)$ with variable $E^{(\zeta)}_{\tau,L}$ in the denominators of terms in the sum of (28) are all different. Therefore, (28) in this case results in a polynomial equation with variable $E^{(\zeta)}_{\tau,L}$. The degree of the polynomial equals exactly to the dimension $\frac{1}{2}(N-\tau-\tau_s)+1$ of the concerned Hilbert subspace. There are exactly $\frac{1}{2}(N-\tau-\tau_s)+1$ distinct roots $E^{(\zeta)}_{\tau,L}$ of (28) in this case. Hence, the model is exactly solved.

III. Fit to the E(5) results

In comparison to the consistent-Q Hamiltonian (1), which describes the U(5)-O(6) phase transition, the EXT is in the U(5) phase when $g_2 = 0$, while there is no pure O(6) phase for finite-N cases even when $\Delta = 0$ and $g_2 \neq 0$. When $\Delta = \lambda = 0$, by using the exact solutions shown in the previous section, the state corresponding to the lowest level for given τ of (20) in this case can simply be written as

$$|N, 1, \tau\alpha L\rangle = \sqrt{\frac{2}{N-\tau-\tau_s+2}} \sum_{\xi=0}^{\frac{1}{2}(N-\tau-\tau_s)} |\xi\rangle \qquad (29)$$

with energy

$$E^{(1)}_{\tau,L} = -\frac{1}{2} g_2 (N-\tau-\tau_s), \qquad (30)$$

while all other excited states for given τ and L are degenerate with $E^{(\zeta\neq 1)}_{\tau,L} = 0$, of which the corresponding eigenstates are not provided by the exact solution shown in (28). The results shown in (29) and (30) are only relevant to nuclear system in the large-N limit with equidistant spectrum in τ: $E^{(1)}_{1,2} - E^{(1)}_{0,0} = E^{(1)}_{2,L} - E^{(1)}_{0,0} = g_2$, $E^{(1)}_{3,L} - E^{(1)}_{0,0} = E^{(1)}_{4,L} - E^{(1)}_{0,0} = 2g_2$, $\cdots$, where the situation is quite similar to the spectrum in the O(6) limit after adding the Casimir operators (20) of the subalgebras $O(5) \supset O(3)$ as is done in [4] for the E(5) model.

According to the concept of quasidynamical symmetry [22–26], the system described by the consistent-Q Hamiltonian (1) remains in the U(5) phase until the control parameter reaches the critical point. Since the EXT is only used to describe the phase transition from the U(5) phase to the E(5)-like critical point in the IBM, this is what we intend here as well. Anyway, when all parameters in (20) are nonzero, the system remains within the U(5)-O(6) transitional phase since the seniority number τ of the common subgroup O(5) is always a good quantum number of the system. In this case, the system, similar to that described by the consistent-Q Hamiltonian, remains in the U(5) (vibrational) quasidynamical symmetry phase when g_2 is small, while the E(5) model results can be better described by the EXT with the increasing of g_2. In this section, it will be shown that the Hamiltonian (20) is indeed suitable to describe nuclei around the E(5) critical point when N is small.

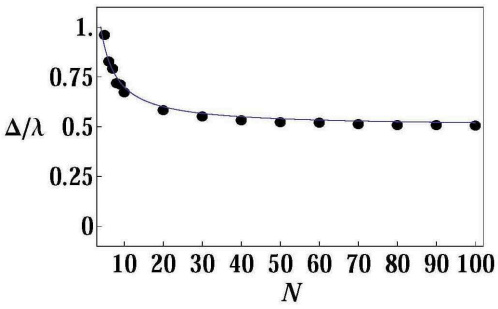

FIG. 1: The ratio of the parameters Δ/λ used in the fits as a function of N.

In the original E(5) model [4], the excitation energies $E^{(\zeta)}_{\tau,L} - E^{(1)}_{0,0}$ are determined by the ζ-th zero of the Bessel function $J_{\tau+3/2}(z)$, which are L-independent. For any reasonable value of N, we shall compare fitting results of the EXT with those of the E(5) model up to the level of $\zeta = 4$ and $\tau = 1$. In the fitting, the energies are in unit of the energy of the first excited state, $E^{(1)}_{1,2} - E^{(1)}_{0,0}$. It is known that nuclei at or near the E(5) critical point are in the vibration to γ-soft transitional region with mass number $A \sim 100$–130, of which the boson number in the IBM is always small with $N \sim 5$–10. In fitting the low-lying level energies of the E(5) model, we fix the parameter g_2 to be a nonzero scale factor and adjust parameters Δ and λ in (20), from which the best fits to the E(5) model results were obtained. The fitting results of the level energies are shown in Table I, in which the corresponding level energies obtained from the consistent-Q IBM Hamiltonian at the critical point (CQ) were also provided. We observe that the ratio of the parameters Δ and λ must be within a reasonable range with $\Delta/\lambda \sim 0.5$–1.0 as shown in Fig. 1, and the magnitude of Δ and λ relative to g_2 should not be too large in order to reproduce the best fit not only to the level energies, but also to the $B(E2)$ values. These parameters used in the fits are shown in Table II. In the fitting, the E2 transition operator is simply chosen as

$$\hat{T}^{(E2)}_q = e_2 (s^\dagger \tilde{d} + d^\dagger \tilde{s})^2_q, \qquad (31)$$

where e_2 is the boson effective charge, which is a global scale and is fixed to give $B(E2, 2^+_1 \to 0^+_1) = 100$ in all cases.

In the fitting,

$$\chi^2 = \frac{1}{N^{E(5)} - N^{par}} \sum_{i=1}^{N^{E(5)}} (X^{E(5)}_i - X_i)^2 \qquad (32)$$

is used, where $N^{E(5)}$ is the number of data taken from the E(5)

model used in the fitting, N^{par} is the number of parameters in the model, and X_i is a level energy obtained from either the EXT or the CQ corresponding to $X_i^{E(5)}$ in the E(5) model. Since the energies are in unit of $E_{1,2}^{(1)} - E_{0,0}^{(1)}$ and the ground state energy is thus set to be zero, the energies of the ground and the first excited level are not included in (32). As the consequence, the number of parameters in the EXT are 2, while there is no free parameter in the CQ. Once the level energies are fit, the B(E2) values are fixed. In the EXT, we adjust the parameters to keep

$$\chi^2_{E2} = \frac{1}{N^{E(5)}(E2)} \sum_{i=1}^{N^{E(5)}(E2)} (X_i^{E(5)}(E2) - X_i(E2))^2 \qquad (33)$$

less than that of the CQ and then to keep χ^2 to be as small as possible, where $N^{E(5)}(E2)$ is the number of B(E2) values taken from the E(5) model used in the fitting, $X_i(E2)$ is a B(E2) value obtained from either the EXT or the CQ corresponding to $X_i^{E(5)}(E2)$ in the E(5) model. The fitted B(E2) values are those among the low-lying excited states shown in [15] except $B(E2,4_4^+ \to 2_3^+)$ and $B(E2,0_4^+ \to 2_3^+)$ between relatively higher excited states, where we use 0_1^+ ($\zeta=1,\tau=0$), 2_1^+ ($\zeta=1,\tau=1$), 2_2^+ and 4_1^+ ($\zeta=1,\tau=2$), 0_ζ^+ ($\zeta=2,\tau=0$), 0_τ^+, 3_1^+, 4_2^+, and 6_1^+ ($\zeta=1,\tau=3$), 2_3^+ ($\zeta=2,\tau=1$), 4_4^+ ($\zeta=2,\tau=2$), and 0_4^+ ($\zeta=3,\tau=0$) to label the corresponding excited states in the models. Though $B(E2,4_4^+ \to 2_3^+)$ and $B(E2,0_4^+ \to 2_3^+)$ are listed for comparison, they are excluded in χ^2_{E2} because these two values do not approach to the corresponding E(5) results with the increasing of N. Moreover, $B(E2,2_2^+ \to 0_1^+)$, $B(E2,4_2^+ \to 2_1^+)$, $B(E2,0_\tau^+ \to 2_1^+)$, and $B(E2,2_1^+ \to 0_1^+)$ are also excluded in χ^2_{E2} since the former three B(E2) values are obviously zero, while $B(E2,2_1^+ \to 0_1^+) = 100$ is set for all the cases studied.

As shown in Table I, not only the first a few low-lying level energies, but also the existing higher-lying level energies up to $\xi = 4$ and $\tau = 1$ produced by the EXT are in good agreement with those of E(5) model. Actually, all excitation energies obtained from the EXT are much closer to the corresponding E(5) results though they are not fully listed in Table I. It is obvious that the CQ results are globally worse due to the fact that the higher lying levels produced by the CQ are too low in energy in comparison to the corresponding E(5) results. Some $B(E2)$ values of the transitions among the low-lying states in the model in comparison with the corresponding E(5) results and those in the CQ are shown in Table III. It can be observed in Table III that these transitional rates increase with the increasing of N, of which the pattern is similar to that produced by the CQ. These transitional rates become closer to the corresponding E(5) results with the increasing of N except $B(E2,0_4^+ \to 2_3^+)$ not included in (33), which is about 1.5 times larger than the corresponding E(5) value when $N = 10$. Except $B(E2,0_4^+ \to 2_3^+)$, other $B(E2)$ values of the EXT are slightly closer to the corresponding E(5) results than those of the CQ with the increasing of N for $N = 5$–10.

Similar to the CQ [14], of which the Hamiltonian (1) can be diagonalized easily, large-N cases of the EXT can also be worked out. We present results of the low-lying level energies and the reduced E2 transitional rates of the model with $N = 1000$ bosons in Tables IV and V, respectively. Since numerical results of the IBM fit to the E(5) results with $N = 60$ are also available [15], the EXT results with $N = 60$ are also shown in Tables IV and V in comparison with the corresponding results of the IBM fit provided in [15]. It can be observed from Table IV that the EXT results are always better than those of the CQ, especially for higher excited states. In fact, the tendency that higher levels become too low in energy in the CQ in comparison to the corresponding E(5) results is not altered in the IBM fits shown in [15], while it is overcome in the EXT. The quality of the EXT fit becomes better with the increasing of N when $N \leq 60$. However, similar to the CQ, both χ^2 and χ^2_{E2} of the EXT also increase with the increasing of N when N is sufficiently large. It is clearly shown in Table V that the reduced E2 transitional rates is closest to the corresponding E(5) results when $N = 60$ except $B(E2,4_4^+ \to 2_3^+)$ and $B(E2,0_4^+ \to 2_3^+)$, which are about 1.45 and 2.22 times larger than the corresponding E(5) results, respectively. With the increasing of N, e. g., $N = 1000$, these transitional rates all become larger than the corresponding E(5) results, but closer to those of the E(5)-β^{2n} model with $n \geq 2$ shown in Table V of Ref. [15]. Anyway, the EXT does not provide with results of the E(5) model in finite-N cases.

IV. The classical energy surface

The classical limit of the IBM may be found by using the coherent state or intrinsic state formulism [16, 17, 27]. Usually, the ground state of a system described by the IBM is written as a condensate of bosons with

$$|c\rangle = \sqrt{\frac{1}{N!}} \left(\Gamma_c^\dagger\right)^N |0\rangle, \qquad (34)$$

where

$$\Gamma_c^\dagger = \frac{1}{\sqrt{1+\beta^2}} \left(s^\dagger + \beta\cos\gamma d_0^\dagger + \frac{1}{2}\beta\sin\gamma(d_2^\dagger + d_{-2}^\dagger) \right), \qquad (35)$$

in which the parameters β and γ are Bohr variables defined in the classical limit of the IBM. By using the method proposed in [27], it can easily be found that

$$\langle c|\hat{n}_d|c\rangle = \frac{N\beta^2}{1+\beta^2}, \qquad (36)$$

and

$$\langle c|\hat{P}^\dagger\hat{P}|c\rangle = \frac{N(N-1)}{4(1+\beta^2)^2}(1-\beta^2)^2, \qquad (37)$$

with which one can observe that the critical point of the U(5)–O(6) phase transition described by the CQ Hamiltonian is at

$x = 1/2$ in the large-N limit since there is a minimum in the energy surface at $\beta = 0$ and $\partial^2 E(\beta,\gamma)/\partial\beta^2 = 0$ at $\beta = 0$ when $x = 1/2$. This type of analysis shows that the U(5)–O(6) phase transition is of the second order, and the energy surface is independent of γ since the system is γ unstable.

However, the operators $\tilde{S}^+_\rho$ and $\tilde{S}^-_\rho$ used in the third term of (20) are only well defined in the $U(6) \supset U(5) \supset O(5)$ basis, and there is the O(5) seniority number τ mixing in the coherent state $|c\rangle$. Therefore, one can not derive the energy surface described by (20) in the classical limit using (34) or using the method proposed in [27] directly. Moreover, since the quantum number of the angular momentum is also not a good quantum number in (34), the coherent state (34) may be expanded in terms of any complete set of $U(6) \supset U(5) \supset O(5)$ basis vectors for given N. Due to the multiplicity occurring in the $O(5) \downarrow O(3)$ reduction, we expand (34) in terms of the $U(6) \supset U(5) \supset O(5) \supset O_1(3) \otimes U(1) \supset O_1(2) \otimes U(1)$ basis vectors [28], which are orthonormal and multiplicity-free. Specifically, for given N, n_d, and τ, the $U(6) \supset U(5) \supset O(5) \supset O_1(3) \otimes U(1) \supset O_1(2) \otimes U(1)$ basis vectors may be expressed as [28]

$$|N, n_d, \tau, r, m_r, m_J\rangle = \left(\frac{(2\tau+3)!!}{(N-n_d)!(\frac{n_d-\tau}{2})!(n_d+\tau+3)!!}\right)^{1/2} \times s^{\dagger N-n_d} P_2^{\dagger\frac{n_d-\tau}{2}} \sum_{\eta=0}^{t/2} \left(\frac{2^{r+m_r}(2r+1)!!(r+m_r)!(r-m_r)!r!}{\eta!(2r+2\eta+1)!!(2r)!}\right)^{\frac{1}{2}} P_1^{\dagger\eta} \times b_\eta^{\tau,t,r,m_J} \sum_x \frac{d_1^{\dagger x} d_0^{\dagger r+m_r-2x} d_{-1}^{\dagger x-m_r}}{2^x (x-m_r)!(r+m_r-2x)!x!} \left| \begin{matrix} |m_J| + t/2 - \eta \\ m_J \end{matrix} \right\rangle \quad (38)$$

with $\tau = r + 2|m_J| + t$, where $t = 0, 2, 4, \cdots$, r can be taken as zero or positive integer, the U(1) quantum number m_J can be taken as zero, integer, or half-integer, the $O_1(2)$ quantum number $m_r = r, r-1, \cdots, -r$ for given $O_1(3)$ quantum number r,

$$P_2^\dagger = \sqrt{2} P^\dagger, \;\; P_1^\dagger = \frac{1}{\sqrt{2}} \left(2 d_1^\dagger d_{-1}^\dagger - d_0^{\dagger\,2}\right), \quad (39)$$

$$b_\eta^{\tau,t,r,m_J} = \left[\frac{(2\tau+1-t)!!\;(4|m_J|+t)!!\;(2r+t+1)!!\;t!!}{(2\tau+1)!!\;(4|m_J|+t-2\eta)!!\;(2\eta)!!\;(2r+2\eta+1)!!\;(t-2\eta)!!}\right]^{\frac{1}{2}}, \quad (40)$$

and

$$\left| \begin{matrix} |m_J| + t/2 - \eta \\ m_J \end{matrix} \right\rangle = \begin{cases} \frac{d_2^{\dagger\,2|m_J|+t/2-\eta} d_{-2}^{\dagger\,t/2-\eta}}{\sqrt{(2|m_J|+t/2-\eta)!(t/2-\eta)!}}|0\rangle \;\; \text{for} \;\; m_J \geq 0, \\ \frac{d_2^{\dagger\,t/2-\eta} d_{-2}^{\dagger\,2|m_J|+t/2-\eta}}{\sqrt{(2|m_J|+t/2-\eta)!(t/2-\eta)!}}|0\rangle \;\; \text{for} \;\; m_J < 0. \end{cases} \quad (41)$$

For given N, by using the $U(6) \supset U(5) \supset O(5) \supset O_1(3) \otimes U(1) \supset O_1(2) \otimes U(1)$ basis vectors shown in (38), expectation value of any operator $\hat{O}$ under the intrinsic state (34) may be expressed as

$$\langle c|\hat{O}|c\rangle = \sum \langle N, n_d, \tau, r, m_r, m_J|\hat{O}|N, n'_d, \tau', r', m'_r, m'_J\rangle \langle c|N n_d \tau r\; m_r m_J\rangle \langle c|N n'_d \tau' r' m'_r m'_J\rangle, \quad (42)$$

where the summation should run over all possible n_d, τ, r, m_r, m_J and $n'_d, \tau', r', m'_r, m'_J$. Since the Hamiltonian (20) keeps τ unchanged, and is independent of quantum numbers of the $O(5)$ subgroups, (42) can be simplified as

$$\langle c|\hat{O}|c\rangle = \sum_{n_d, n'_d, \tau} O^{N,\tau}_{n_d, n'_d} \times \sum_{r, m_r, m_J} \langle c|N n_d \tau r\; m_r m_J\rangle \langle c|N n'_d \tau r\; m_r m_J\rangle \quad (43)$$

when $\hat{O}$ is any term in (20), where $O^{N,\tau}_{n_d,n'_d} \equiv \langle N n_d \tau r\; m_r m_J|\hat{O}|N n'_d \tau r\; m_r m_J\rangle$. The real expansion coefficient $\langle c|N n_d \tau r\; m_r m_J\rangle$ can be obtained by using the explicit form shown in (34), (38), and the method proposed in [27].

Generally speaking, the classical limit should be defined in the infinite N limit. Though analytical expression of (43) in terms of arbitrary N is impossible, one can numerically calculate (43) for finite N cases. For example, one can verify that the expressions shown in (36) and (37) are indeed valid by using (43) and the basis vectors shown in (38). The matrix elements of $\hat{H}_{\rm ext} = -g_2 \sum_{k=1}^{\infty} (\tilde{S}_s^{+k} \tilde{S}_d^{-k} + \tilde{S}_d^{+k} \tilde{S}_s^{-k})$ appearing in (20) can then be expressed simply as

$$\left(\hat{H}_{\rm ext}\right)^{N,\tau}_{n_d,n'_d} = \begin{cases} 0, & \text{when} \;\; n_d = n'_d, \\ -g_2, & \text{when} \;\; n_d \neq n'_d. \end{cases} \quad (44)$$

We have verified numerically that

$$\langle c|\hat{H}_{\rm ext}|c\rangle = -g_2 \frac{1}{(1+\beta^2)^N} f_{N-1}(\beta^2), \quad (45)$$

which is indeed γ-independent, where $f_{N-1}(\beta^2)$ is a polynomial in β^2 of degree $N-1$. Thus, we calculated $\langle c|\hat{H}_c|c\rangle$ using the explicit form shown in (34) and (38) for some finite N cases with the parameters of (20) in fitting the E(5) results. When $N = 10$ for example, we obtain

$$u(\beta) = \langle c|\hat{H}_c|c\rangle = \Delta \frac{N\beta^2}{1+\beta^2} + \lambda \frac{(N-1)(1-\beta^2)^2}{4(1+\beta^2)^2} + \lambda \frac{(N-1)\beta^2}{2(1+\beta^2)^2} - g_2 (6\beta^2 + 53.84\beta^4 + 207.8\beta^6 + 453.7\beta^8 + 617.2\beta^{10} + 538.7\beta^{12} + 295.9\beta^{14} + 93.7\beta^{16} + 13.2\beta^{18})/(1+\beta^2)^{10} \quad (46)$$

with the parameters shown in Table II for the $N = 10$ case, which answers why the results of the EXT are in between those of the E(5)-β^{2n} models in the large N cases shown in the previous section. Actually, the B(E2) values $B(E2, 4_4^+ \to 2_3^+)$ and $B(E2, 0_4^+ \to 2_3^+)$ in the EXT are indeed close to those of the E(5)-β^{2n} models with $n = 2$ or $n = 3$ when $N = 60$ as shown in [15]. Fig. 2 shows various potential energy surfaces

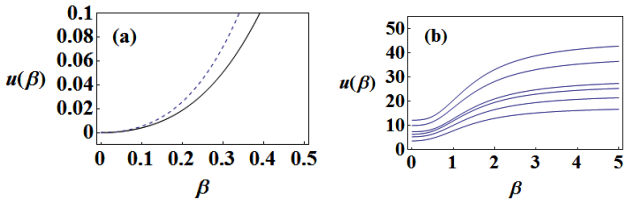

FIG. 2: (Color online) Panel (a) shows potential energy surface (in unit of $10g_2$) of the EXT (solid curve) and that derived from the CQ in unit of $g = g_2$ (dashed curve) as functions of β with $N = 10$, where the potential energy is set with $u(0) = 0$, while panel (b) shows potential energy surfaces (in unit of g_2) as functions of β for various N cases, in which the curves from bottom to the top are those with $N = 5$–10, respectively.

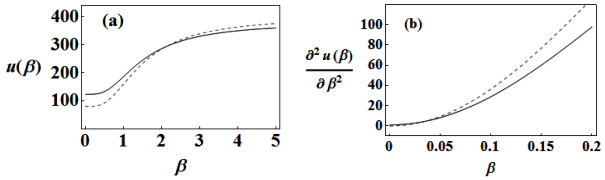

FIG. 3: (Color online) Panel (a) shows potential energy surface (in unit of g_2) of the EXT (solid curve) and that derived from the CQ in unit of $g = g_2/40$ (dashed curve) as functions of β with $N = 16$, while panel (b) shows the second derivative of $u(\beta)$ at and near $\beta = 0$ with the same conditions as indicated for the left panel.

in unit of g_2 as function of β, which is typical for nuclei near or at the E(5) critical point. These energy potential surfaces have been determined by using the parameters of (20) in fitting the E(5) results for these N cases shown previously. In order to compare the energy surface derived from the EXT with that of the CQ, Fig. 3 shows the energy surface for the $N = 16$ case of the EXT in unit of g_2 and that derived from the CQ, of which the latter is derived from (1) with $g = g_2/40$ and $x = 1/2$. The results show that, even though the two descriptions are different, they behavior similarly in the classical limit. Most importantly, similar to the CQ, the energy surface of the EXT indeed presents a single minimum at $\beta = 0$ and satisfies the condition $\left(\partial^2 u(\beta)/\partial\beta^2\right)_{\beta=0} = 0$ as shown in Fig 3.

In order to find exact critical point in the EXT, we rewrite the Hamiltonian (20) as

$$\hat{H}_{\rm c} = \Delta\hat{n}_d + \frac{\lambda}{N}(S_s^+ S_s^- + S_d^+ S_d^-) - z\, g_2 \sum_{k=1}^{\infty}(\tilde{S}_s^{+k}\tilde{S}_d^{-k} + \tilde{S}_d^{+k}\tilde{S}_s^{-k}). \quad (47)$$

Actually, similar to the CQ, the position of the critical point will be different when the scale of the parameters in the model is changed. In present analysis, we use (47) with $z = 1.0$ to fit the E(5) results by adjusting the parameters Δ and λ in unit of g_2. Then, for given N, Δ, and λ, the critical point value of the dimensionless parameter z can easily be determined. We found the critical point value of z always satisfies $z_{\rm c} \geq 1.0$ when N is finite, which approaches to 1.0 in the large N limit. We have verified that $\left(\partial^2 u(\beta)/\partial\beta^2\right)_{\beta=0,z>z_{\rm c}} > 0$, $\left(\partial^2 u(\beta)/\partial\beta^2\right)_{\beta=0,z<z_{\rm c}} < 0$, and $\left(\partial^2 u(\beta)/\partial\beta^2\right)_{\beta=0,z=z_{\rm c}} = 0$, which shows the phase transition in the EXT is also of the second order. When $z \leq z_{\rm c}$ the model is in the spherical (U(5)) to the E(5)-like critical point phase, while the model with $z \gg z_{\rm c}$ may be not physical for finite N cases, and is not studied in this paper. For simplicity, we always set $z = 1.0$ in the fitting shown in Sec. III, which ensures the model in the fitting always remain in the U(5) to the E(5) like critical point phase. In conclusion, the E(5) results can be approximately described by the EXT in U(5) to the E(5)-like critical point phase with results better than the CQ description.

V. Comparison with experimental results

As shown in [29], there are many nuclei in $A = 100$–130 mass region near the E(5) critical point. It was confirmed in [9] that ^{102}Pd, ^{104}Ru, and ^{116}Cd are good candidates near the E(5) critical point. In this section, we use the EXT to fit low-lying energy levels and some B(E2) values for ^{102}Pd ($N = 5$), ^{134}Ba ($N = 5$), ^{128}Xe ($N = 6$), ^{104}Ru ($N = 8$), ^{108}Pd ($N = 8$), ^{116}Cd ($N = 8$), and ^{114}Cd ($N = 9$). The levels of the nuclei fitted have been confirmed in experiment with relatively abundant B(E2) data except ^{128}Xe, of which only four B(E2) values are available. These nuclei have also been well studied in the original E(5) model [5–8], the model with the sextic type potential in β [9], and the confined γ-soft rotor model [11]. The fitting results of the EXT and the CQ to the level energies and experimentally deduced B(E2) values for these nuclei are shown in Tables VII and VIII, in which the fitting results of the model with the sextic potential in β (SET) shown in [9] for ^{102}Pd, ^{104}Ru, ^{108}Pd, ^{116}Cd, and ^{114}Cd are also provided for comparison. The quantities χ^2 and χ^2_{E2} are used to measure the quality of the fits, which are calculated from (32) and (33), respectively, with $N^{E(5)}$, $X_i^{E(5)}$, $N^{E(5)}(E2)$, and $X_i^{E(5)}(E2)$ being replaced by the corresponding experimental data. As shown in Tables VII-IX, the level patterns of ^{102}Pd and ^{128}Xe are closest to the SET and the E(5) prediction, respectively, while their B(E2) values are best fitted by the E(5) and the EXT, respectively, from which ^{102}Pd may be recognized as the best E(5) candidate. The overall fitting quality is measured by the average of χ^2 and χ^2_{E2} over these seven nuclei as listed in Table X, from which we conclude that these nuclei are best fitted by the EXT. It can be expected that the EXT should fit the vibration to γ-soft transitional nuclei much better than the CQ if higher excited levels are taken into account though we did not done so in this paper due to in lack of experimental data of relatively higher excited states.

VI. Summary

In this paper, an alternative solvable extended Hamiltonian that includes multi-pair interactions among s- and d-bosons

up to infinite order within the framework of the interacting boson model is proposed to provide a better description of the E(5) model results for finite-N cases. Numerical fits to low-lying level energies and B(E2) values of the E(5) model for various N cases were carried out to test the theory. The results show that the extended Hamiltonian within the IBM provides a better description of the E(5) model results, especially when higher excited states are taken into account. However, B(E2) values of the transitions among higher excited states, e. g., $B(E2,4_4^+ \to 2_3^+)$ and $B(E2,0_4^+ \to 2_3^+)$, do not approach the corresponding E(5) results with increasing N. Moreover, similar to the results of the consistent-Q formalism, the χ^2 and χ^2_{E2} increase with the increasing of N. Specifically, the results of the extended model proposed in this paper do not approach to those of the E(5) model in the large-N limit, but approach to those of the E(5)-β^{2n} model with $n \geq 2$ studied in [15], for example when $N = 60$. And indeed, as analyzed by using the coherent state method, the classical energy surface of the extended model can be described by a polynomial function of β^2. Low-lying level energies and B(E2) values of the transitions among these levels for ^{102}Pd, ^{134}Ba, ^{128}Xe, ^{104}Ru, ^{108}Pd, and ^{114,116}Cd are fitted by the extended model and compared with the results of the E(5) model and those of the consistent-Q formalism. The overall fitting results show that these nuclei are best fitted by the EXT. It can be expected that the extended model should fit the vibration to γ-soft transitional nuclei much better than the original consistent-Q formalism if higher excited states are taken into account, which will be our future work when experimental data for higher excited states, especially the relevant B(E2) values of nuclei in the U(5)-O(6) transitional region are available.

Acknowledgments

Support from U.S. National Science Foundation (OCI-0904874), Southeastern Universities Research Association, the Natural Science Foundation of China (11175078, 11375080, 11375005, 11005056), and the LSU–LNNU joint research program (9961) is acknowledged.

[1] S. Sachdev, *Quantum Phase Transitions* (Cambridge Univ. Press, Cambridge, 1999).
[2] A. Bohr and B. R. Mottelson, *Nuclear Structure Vol. I* (Benjamin, New York, 1969); *Vol. II* (Benjamin, New York, 1975).
[3] F. Iachello and A. Arima, *The Interacting Boson Model* (Cambridge University, Cambridge, England, 1987).
[4] F. Iachello, Phys. Rev. Lett. 85, 3580 (2000).
[5] R. F. Casten and N. V. Zamfir, Phys. Rev. Lett. 85, 3584 (2000).
[6] A. Frank, C. E. Alonso, and J. M. Arias, Phys. Rev. C 65, 014301 (2001).
[7] N. V. Zamfir, M. A. Caprio, R. F. Casten, C. J. Barton, C. W. Beausang, Z. Berant, D. S. Brenner, W. T. Chou, J. R. Cooper, A. A. Hecht, R. Kručken, H. Newman, J. R. Novak, N. Pietralla, A. Wolf, and K. E. Zyromski, Phys. Rev. C 65, 044325 (2002).
[8] Da-li Zhang and Yu-xin Liu, Phys. Rev. C 65, 057301 (2002).
[9] G. Lévai and J. M. Arias, Phys. Rev. C 81, 044304 (2010).
[10] G. Lévai and J. M. Arias, Phys. Rev. C 69, 014304 (2004).
[11] D. Bonatsos, D. Lenis, N. Minkov, P. P. Raychev, and P. A. Terziev, Phys. Rev. C 69, 044316 (2004).
[12] F. Pan and J. P. Draayer, Nucl. Phys. A636, 156 (1998).
[13] J. M. Arias, C. E. Alonso, A. Vitturi, J. E. García-Ramos, J. Dukelsky, and A. Frank, Phys. Rev. C 68, 041302(R) (2003).
[14] J. E. García-Ramos, J. Dukelsky, and J. M. Arias, Phys. Rev. C 72, 037301 (2005).
[15] J. E. García-Ramos and J. M. Arias, Phys. Rev. C 77, 054307 (2008).
[16] J. N. Ginocchio and M. W. Kirson, Nucl. Phys. A 350, 31 (1980).
[17] A. E. L. Dieperink, O. Scholten,and F. Iachello, Phys. Rev. Lett. 44, 1747 (1980).
[18] A. Klein and M. Vallières, Phys. Rev. Lett. 46, 586 (1981).
[19] F. Pan, Y. Zhang, and J. P. Draayer, J. Phys. G 31, 1039 (2005).
[20] F. Pan, V. G. Gueorguiev, and J. P. Draayer, Phys. Rev. Lett. 92, 112503 (2004).
[21] F. Pan, B. Li, Y.-Z. Zhang, and J. P. Draayer, Phys. Rev. C 88, 034305 (2013).
[22] D. J. Rowe, Phys. Rev. Lett. 93, 122502 (2004).
[23] D. J. Rowe, P. S. Turner, and G. Rosensteel, Phys. Rev. Lett. 93, 232502 (2004).
[24] D. J. Rowe, Nucl. Phys. A745, 47 (2004).
[25] D. J. Rowe and G. Thiamanova, Nucl. Phys. A760, 59 (2005).
[26] P. S. Turner and D. J. Rowe, Nucl. Phys. A756, 333 (2005).
[27] P. Van Isacker and J.-Q. Chen, Phys. Rev. C 24, 684 (1981).
[28] Feng Pan, Lina Bao, Yao-Zhong Zhang, J. P. Draayer, Eur. Phys. J. Plus 129 (2014) 169.
[29] R. M. Clark, M. Cromaz, M. A. Deleplanque, M. Descovich, R. M. Diamond, P. Fallon, I. Y. Lee, A. O. Macchiavelli, H. Mahmud, E. Rodriguez-Vieitez, F. S. Stephens, and D. Ward, Phys. Rev. C 69, 064322 (2004).
[30] A. A. Sonzogni, Nucl. Data Sheets 103, 1 (2004).
[31] H. Miyahara, H. Matumoto, G. Wurdiyanto, K. Yanagida, Y. Takenaka, A. Yoshida, and C. Mori, Nucl. Instr. Methods A 353, 229 (1994).
[32] J. Stachel et al., Nucl. Phys. A 419, 589 (1984).
[33] M. Luontama et al., Z. Phys. A 324, 317 (1986).
[34] J. Blachot, Nucl. Data Sheets 108, 2035 (2007).
[35] J. Blachot, Nucl. Data Sheets 81, 599 (1997).
[36] J. Blachot, Nucl. Data Sheets 97, 593 (2002).
[37] P. E. Garrett, K. L. Green, and J. L. Wood, Phys. Rev. C 78, 044307 (2008).
[38] J. Blachot, Nucl. Data Sheets 92, 455 (2001).

TABLE I: Comparison of low-lying level energies generated by the extended IBM Hamiltonian (EXT) and the IBM consistent-Q Hamiltonian at the critical point with $x = 1/2$ (CQ) for serval values of N with those provided by the E(5) model, where "—" denotes that the corresponding level in the IBM does not exist due to the fact that N is finite.

ζ, τ	E(5)	EXT						CQ					
		N=5	N=6	N=7	N=8	N=9	N=10	N=5	N=6	N=7	N=8	N=9	N=10
1, 0	0.00	0.00	0.00	0.00	0.00	0.00	0.00	0.00	0.00	0.00	0.00	0.00	0.00
1, 1	1.00	1.00	1.00	1.00	1.00	1.00	1.00	1.00	1.00	1.00	1.00	1.00	1.00
1, 2	2.20	2.19	2.12	2.20	2.12	2.19	2.13	2.15	2.15	2.15	2.14	2.14	2.14
2, 0	3.03	3.14	3.19	3.33	3.34	3.38	3.37	3.18	3.10	3.04	3.00	2.96	2.92
1, 3	3.59	3.50	3.46	3.52	3.46	3.51	3.47	3.43	3.42	3.42	3.41	3.40	3.40
2, 1	4.80	4.74	4.83	4.97	4.98	4.99	5.02	4.70	4.59	4.51	4.45	4.40	4.35
1, 4	5.17	5.02	4.92	5.08	4.93	5.03	4.96	4.82	4.79	4.78	4.77	4.76	4.76
2, 2	6.78	6.56	6.63	6.83	6.80	6.82	6.86	6.30	6.17	6.06	5.99	5.92	5.87
3, 0	7.58	7.41	7.58	7.79	7.82	7.79	7.88	7.13	6.93	6.79	6.67	6.58	6.50
1, 5	6.93	6.64	6.62	6.75	6.64	6.69	6.67	6.30	6.27	6.25	6.23	6.21	6.20
1, 6	8.88	—	8.44	8.67	8.49	8.57	8.53	—	7.82	7.79	7.76	7.74	7.72
2, 3	8.97	8.49	8.67	8.85	8.85	8.81	8.91	7.98	7.82	7.70	7.60	7.53	7.45
3, 1	10.11	9.66	9.95	10.16	10.24	10.13	10.31	9.05	8.81	8.72	8.49	8.37	8.27
2, 4	11.36	—	10.83	11.09	11.07	11.02	11.15	—	9.55	9.41	9.29	9.20	9.11
3, 2	12.85	—	12.48	12.76	12.83	12.69	12.93	—	10.75	10.52	10.36	10.21	10.09
4, 0	13.64	—	13.40	13.68	13.81	13.62	13.92	—	11.42	11.15	10.95	10.78	10.64
2, 5	13.95	—	—	13.47	13.52	13.38	13.60	—	—	11.18	11.05	11.00	10.84
3, 3	15.81	—	—	15.49	15.65	15.41	15.76	—	—	12.48	12.28	12.11	11.97
2, 6	16.73	—	—	—	16.11	15.97	16.21	—	—	—	12.87	12.74	12.63
4, 1	16.93	—	—	16.78	17.01	16.69	17.13	—	—	13.31	13.06	12.86	12.69
χ^2		0.08	0.08	0.04	0.07	0.09	0.06	0.18	0.30	0.43	0.48	0.51	0.53

TABLE II: Parameters of the EXT used in the fitting.

	Δ/g_2	λ/g_2
$N = 5$	2.90	2.91
$N = 6$	3.00	3.56
$N = 7$	2.93	3.66
$N = 8$	3.10	4.26
$N = 9$	3.24	4.45
$N = 10$	3.69	5.42
$N = 60$	15.70	29.74
$N = 1000$	333.80	665.40

TABLE III: Some B(E2) values in the EXT and the CQ for serval values of N compared with those provided by the E(5) model, where the B(E2) values with $*$ are not included in χ^2_{E2}.

	E(5)	EXT						CQ					
		N=5	N=6	N=7	N=8	N=9	N=10	N=5	N=6	N=7	N=8	N=9	N=10
$B(E2:2_1^+\to 0_1^+)$	100	100	100	100	100	100	100	100	100	100	100	100	100
$B(E2:4_1^+\to 2_1^+)$	167.4	148.7	152.3	155.6	156.4	159.2	160.4	140.8	147.2	151.4	154.7	157.2	159.2
$B(E2:6_1^+\to 4_1^+)$	216.9	157.6	174.2	182.9	189.4	195.4	200.8	143.8	161.7	173.2	181.9	188.7	194.2
$B(E2:2_2^+\to 2_1^+)$	167.4	148.7	152.3	155.6	156.4	159.2	160.4	140.8	147.2	151.4	154.7	157.2	159.2
$B(E2:2_2^+\to 0_1^+)$	0.0	0.0	0.0	0.0	0.0	0.0	0.0	0.0	0.0	0.0	0.0	0.0	0.0
$B(E2:4_2^+\to 2_1^+)$	0.0	0.0	0.0	0.0	0.0	0.0	0.0	0.0	0.0	0.0	0.0	0.0	0.0
$B(E2:4_2^+\to 2_2^+)$	113.6	82.5	91.2	95.8	99.2	102.4	105.2	75.3	84.7	90.7	95.3	98.8	101.7
$B(E2:4_2^+\to 4_1^+)$	103.3	75.0	82.9	87.1	90.2	93.1	95.6	68.5	77.0	82.5	86.6	89.8	92.5
$B(E2:3_1^+\to 2_2^+)$	154.9	112.5	124.4	130.6	135.3	139.6	143.5	102.7	115.5	123.7	129.9	134.8	138.7
$B(E2:3_1^+\to 4_1^+)$	62.0	45.0	49.8	52.3	54.1	55.8	57.4	41.1	46.2	49.5	52.0	53.9	55.4
$B(E2:0_\tau^+\to 2_2^+)$	216.9	157.6	174.2	182.9	189.4	195.4	200.8	143.8	161.7	173.2	181.9	188.7	194.2
$B(E2:0_\tau^+\to 2_1^+)$	0.0	0.0	0.0	0.0	0.0	0.0	0.0	0.0	0.0	0.0	0.0	0.0	0.0
$B(E2:2_3^+\to 0_\zeta^+)$	72.2	62.7	68.4	69.4	70.6	71.6	74.9	56.6	64.6	69.7	73.4	76.1	79.4
$B(E2:4_4^+\to 2_3^+)^*$	124.3	72.3	95.4	105.6	110.8	117.7	124.0	60.4	85.7	98.1	108.1	115.6	122.2
$B(E2:0_\zeta^+\to 2_1^+)$	86.8	100.2	97.8	99.0	94.3	99.3	99.5	64.5	72.3	77.1	81.1	84.4	87.2
$B(E2:0_4^+\to 2_3^+)^*$	123.2	88.4	134.8	151.8	161.1	172.6	181.5	42.8	83.4	97.0	109.7	119.2	127.2
χ^2_{E2}		10.9	7.9	6.3	5.1	4.1	3.3	13.6	10.2	8.1	6.4	5.2	4.2

TABLE IV: Comparison of low-lying level energies generated by the EXT and the CQ with $N = 60$ and 1000, respectively, and those generated by the IBM fit for $N = 60$ [15] with those provided by the E(5) model, where "—" denotes that the corresponding level energy in the IBM fit was not provided in [15].

ζ, τ	E(5)	EXT		CQ		IBM fit [15]
		N=60	N=1000	N=60	N=1000	N=60
1, 0	0.00	0.00	0.00	0.00	0.00	0.00
1, 1	1.00	1.00	1.00	1.00	1.00	1.00
1, 2	2.20	2.14	2.18	2.12	2.10	2.21
2, 0	3.03	3.59	3.50	2.60	2.45	3.05
1, 3	3.59	3.45	3.55	3.33	3.29	3.61
2, 1	4.80	5.16	5.23	3.91	3.71	4.51
1, 4	5.17	4.93	5.13	4.64	4.56	5.16
2, 2	6.78	6.95	7.19	5.30	5.03	6.11
3, 0	7.58	8.02	8.31	5.68	5.30	6.68
1, 5	6.93	6.59	6.91	6.02	5.89	6.85
1, 6	8.88	8.44	8.91	7.46	7.28	—
2, 3	8.97	8.95	9.37	6.76	6.41	8.67
3, 1	10.11	10.39	10.90	7.24	6.75	8.51
2, 4	11.36	11.15	11.75	8.27	7.85	—
3, 2	12.85	12.96	13.71	8.85	8.25	10.44
4, 0	13.64	13.98	14.79	9.16	8.48	—
2, 5	13.95	13.54	14.36	9.85	9.34	—
3, 3	15.81	15.74	16.73	10.50	9.79	—
2, 6	16.73	16.13	17.18	11.48	10.88	—
4, 1	16.93	17.13	18.23	10.92	10.09	—
χ^2		0.09	0.17	0.75	0.86	0.40

TABLE V: Some B(E2) values in the EXT and the CQ with $N = 60$ and 1000 and those from the IBM fit with $N = 60$ [15] compared with those provided by the E(5) model, where the B(E2) values with $*$ are not included in χ^2_{E2}.

	E(5)	EXT		CQ		IBM fit [15]
		N=60	N=1000	N=60	N=1000	N=60
$B(E2: 2_1^+ \to 0_1^+)$	100	100	100	100	0.00	100
$B(E2: 4_1^+ \to 2_1^+)$	167.4	167.3	176.3	175.8	181.3	165.2
$B(E2: 6_1^+ \to 4_1^+)$	216.9	224.5	246.1	238.1	251.8	215.2
$B(E2: 2_2^+ \to 2_1^+)$	167.4	167.3	176.3	175.8	181.3	165.2
$B(E2: 2_2^+ \to 0_1^+)$	0.0	0.0	0.0	0.0	0.0	0.0
$B(E2: 4_2^+ \to 2_1^+)$	0.0	0.0	0.0	0.0	0.0	0.0
$B(E2: 4_2^+ \to 2_2^+)$	113.6	117.6	128.9	124.7	131.9	112.8
$B(E2: 4_2^+ \to 4_1^+)$	103.3	106.9	117.2	113.4	119.9	102.6
$B(E2: 3_1^+ \to 2_2^+)$	154.9	160.4	175.8	170.0	179.9	153.8
$B(E2: 3_1^+ \to 4_1^+)$	62.0	64.1	70.3	68.0	71.9	61.5
$B(E2: 0_\tau^+ \to 2_2^+)$	216.9	224.5	246.1	238.1	251.8	215.4
$B(E2: 0_\tau^+ \to 2_1^+)$	0.0	0.0	0.0	0.0	0.0	0.0
$B(E2: 2_3^+ \to 0_\zeta^+)$	75.2	75.2	92.7	101.9	109.9	90.2
$B(E2: 4_4^+ \to 2_3^+)^*$	124.3	143.2	175.2	174.8	192.3	152.3
$B(E2: 0_\zeta^+ \to 2_1^+)$	86.8	99.8	124.5	118.6	135.2	81.6
$B(E2: 0_4^+ \to 2_3^+)^*$	123.2	215.4	265.0	208.6	245.0	155.0
χ^2_{E2}		1.9	6.7	5.7	8.8	2.3

TABLE VI: z_c of the EXT defined in (47) for various N cases with the parameters Δ and λ shown in Table II in fitting the E(5) results.

	z_c
$N = 5$	2.413
$N = 6$	1.957
$N = 7$	1.880
$N = 8$	1.640
$N = 9$	1.631
$N = 10$	1.630
$N = 16$	1.053

TABLE VII: Comparison of low-lying level energies and relevant B(E2) values of ^{102}Pd, ^{134}Ba, and ^{128}Xe with those obtained from the EXT, the CQ, the model with the sextic potential in β (SET) [9], and the E(5) model, where the experimental data of ^{102}Pd were taken from [7], those of ^{134}Ba were taken from [5] and [30], those of ^{128}Xe were taken from [31], CQ_N denotes the consistent-Q description at the critical point with N bosons, and "—" denotes that the corresponding B(E2) value was not determined experimentally.

	E(5)	^{102}Pd	EXT	SET	^{134}Ba	EXT	CQ_5	^{128}Xe	EXT	CQ_6
0_1^+	0.00	0.00	0.00	0.00	0.00	0.00	0.00	0.00	0.00	0.00
2_1^+	1.00	1.00	1.00	1.00	1.00	1.00	1.00	1.00	1.00	1.00
2_2^+	2.20	2.76	2.21	2.58	1.93	2.31	2.15	2.29	2.14	2.15
4_1^+	2.20	2.29	2.21	2.58	2.32	2.31	2.15	2.44	2.14	2.15
0_ζ^+	3.03	2.98	2.69	2.92	3.57	2.92	3.18	3.74	3.38	3.10
0_τ^+	3.59	2.87	3.23	3.70	2.91	3.31	3.43	4.44	3.52	3.42
3_1^+	3.59	3.79	3.23	3.70	2.72	3.31	3.43	3.38	3.52	3.42
4_2^+	3.59	3.84	3.23	3.70	3.26	3.31	3.43	3.79	3.52	3.42
6_1^+	3.59	3.72	3.23	3.70	3.66	3.31	3.43	4.11	3.52	3.42
2_3^+	4.80	3.49	3.72	4.14	3.36	3.92	4.70	4.73	5.11	4.59
$B(E2:4_1^+ \to 2_1^+)$	167.4	154.5	143.9	187.8	154.8	141.9	140.8	146.7	151.3	147.2
$B(E2:6_1^+ \to 4_1^+)$	216.9	–	137.5	257.6	–	129.6	143.8	181.6	172.5	161.7
$B(E2:2_2^+ \to 2_1^+)$	167.4	45.0	143.9	187.8	217.2	141.9	140.8	119.4	151.3	147.2
$B(E2:2_2^+ \to 0_1^+)$	0.0	6.0	0.0	0.0	1.25	0.0	0.0	1.6	0.0	0.0
$B(E2:4_2^+ \to 2_1^+)$	0.0	9.0	0.0	0.0	–	0.0	0.0	–	0.0	0.0
$B(E2:4_2^+ \to 2_2^+)$	113.6	136.4	72.0	136.4	–	67.9	75.3	–	90.4	84.7
$B(E2:4_2^+ \to 4_1^+)$	103.3	<24.0	65.5	121.2	–	61.7	68.5	–	82.1	77.0
$B(E2:3_1^+ \to 2_2^+)$	154.9	–	98.2	184.8	12.8	92.5	102.7	–	123.2	115.5
$B(E2:3_1^+ \to 4_1^+)$	62.0	–	39.3	72.7	–	37.0	41.1	–	49.3	46.2
$B(E2:0_\tau^+ \to 2_2^+)$	216.9	291.0	137.5	257.6	–	129.6	143.8	–	172.5	161.7
$B(E2:0_\tau^+ \to 2_1^+)$	0.0	<0.001	0.0	0.0	3.0	0.0	0.0	–	0.0	0.0
$B(E2:2_3^+ \to 0_\zeta^+)$	72.2	–	47.2	109.1	–	43.7	56.6	–	66.8	64.6
$B(E2:0_\zeta^+ \to 2_1^+)$	86.8	39.4	68.5	163.6	41.7	57.3	64.5	–	93.4	72.3

TABLE VIII: The same as Table VII but for ^{104}Ru, ^{108}Pd, and ^{114,116}Cd, where "—" denotes either that the corresponding B(E2) value was not determined experimentally, or that the theoretical value was not provided in [9], the experimental data of ^{104}Ru were taken from [32–34], those of ^{108}Pd were taken from [35], those of ^{114}Cd were taken from [36], and those of ^{116}Cd were taken from [37, 38], CQ_N denotes the consistent-Q description at the critical point with N bosons.

	E(5)	^{104}Ru	EXT	SET	^{108}Pd	EXT	SET	^{116}Cd	EXT	SET	CQ_8	^{114}Cd	EXT	SET	CQ_9
0_1^+	0.00	0.00	0.00	0.00	0.00	0.00	0.00	0.00	0.00	0.00	0.00	0.00	0.00	0.00	0.00
2_1^+	1.00	1.00	1.00	1.00	1.00	1.00	1.00	1.00	1.00	1.00	1.00	1.00	1.00	1.00	1.00
2_2^+	2.20	2.49	2.03	2.22	2.14	2.03	2.20	2.36	2.07	2.66	2.14	2.17	2.00	2.00	2.14
4_1^+	2.20	2.48	2.03	2.22	2.42	2.03	2.20	2.37	2.07	2.66	2.14	2.30	2.00	2.00	2.14
0_ζ^+	3.03	2.76	3.04	2.34	2.43	2.41	2.30	2.69	2.43	3.09	3.00	2.03	2.00	2.00	2.96
0_τ^+	3.59	3.73	3.25	3.27	3.03	3.21	3.23	2.50	3.22	3.80	3.41	2.33	3.00	3.00	3.40
3_1^+	3.59	3.47	3.25	3.27	3.08	3.13	3.23	3.73	3.22	3.80	3.41	3.34	3.00	3.00	3.40
4_2^+	3.59	4.20	3.25	3.27	3.75	3.13	3.23	3.98	3.22	3.80	3.41	3.10	3.00	3.00	3.40
6_1^+	3.59	4.35	3.25	3.27	4.08	3.13	3.23	3.95	3.22	3.80	3.41	3.56	3.00	3.00	3.40
2_3^+	4.80	4.23	4.41	3.66	3.32	3.60	4.36	3.20	3.72	4.41	4.45	2.44	3.00	–	4.40
$B(E2:4_1^+\to 2_1^+)$	167.4	134.5	154.3	195.2	147.5	163.5	–	163.9	175.0	188.1	154.7	199.4	177.8	–	157.2
$B(E2:6_1^+\to 4_1^+)$	216.9	190.4	184.8	276.8	216.2	202.1	–	327.8	215.0	250.7	181.9	382.6	233.3	–	188.7
$B(E2:2_2^+\to 2_1^+)$	167.4	67.3	154.3	195.2	143.4	163.5	–	74.5	175.0	188.1	154.7	70.7	177.8	–	157.2
$B(E2:2_2^+\to 0_1^+)$	0.0	4.8	0.0	0.0	0.01	0.00	0.0	–	0.0	0.0	0.0	–	0.0	0.0	0.0
$B(E2:4_2^+\to 2_1^+)$	0.0	–	0.0	0.0	–	0.0	0.0	–	0.0	0.0	0.0	1.6	0.0	0.0	0.0
$B(E2:4_2^+\to 2_2^+)$	113.6	82.7	96.8	145.2	111.1	105.7	–	–	117.9	131.3	95.3	102.9	122.2	–	98.8
$B(E2:4_2^+\to 4_1^+)$	103.3	45.2	88.0	132.1	60.6	96.2	–	–	107.1	119.4	86.6	54.7	111.1	–	89.9
$B(E2:3_1^+\to 2_2^+)$	154.9	126.8	132.0	198.2	–	144.4	–	181.8	160.7	179.1	129.9	–	166.7	–	134.8
$B(E2:3_1^+\to 4_1^+)$	62.0	27.4	52.8	79.2	–	57.7	–	53.6	62.1	71.6	52.0	–	66.7	–	53.9
$B(E2:0_\tau^+\to 2_2^+)$	216.9	–	184.8	276.8	<36.4	202.1	–	–	225.0	250.7	181.9	408.4	233.3	–	188.7
$B(E2:0_\tau^+\to 2_1^+)$	0.0	–	0.0	0.0	<0.02	0.0	0.0	1.64	0.0	0.0	0.0	0.01	0.0	0.0	0.0
$B(E2:2_3^+\to 0_\zeta^+)$	72.2	60.1	64.3	122.0	119.2	79.5	–	256.3	105.0	104.5	73.4	209.0	108.9	–	76.1
$B(E2:0_\zeta^+\to 2_1^+)$	86.8	42.3	83.7	182.7	105.1	121.8	–	89.4	175.0	158.2	81.1	88.1	177.8	–	84.4

TABLE IX: χ^2 and χ^2_{E2} values of the models in fitting the low-lying level energies and the B(E2) values shown in Tables VII and VIII for ^{102}Pd, ^{134}Ba, ^{128}Xe, ^{104}Ru, ^{108}Pd, and ^{114,116}Cd.

	^{102}Pd				^{134}Ba			^{128}Xe			^{104}Ru			
	EXT	CQ	E(5)	SET	EXT	CQ	E(5)	EXT	CQ	E(5)	EXT	CQ	E(5)	SET
χ^2	0.20	0.20	0.20	0.16	0.20	0.21	0.24	0.21	0.18	0.16	0.28	0.18	0.16	0.24
χ^2_{E2}	19.4	20.4	19.0	24.2	18.6	20.2	26.3	8.4	8.6	15.8	11.1	11.1	14.2	25.2

	^{108}Pd				^{116}Cd				^{114}Cd		
	EXT	CQ	E(5)	SET	EXT	CQ	E(5)	SET	EXT	CQ	E(5)
χ^2	0.20	0.20	0.23	0.18	0.26	0.23	0.24	0.27	0.19	0.31	0.36
χ^2_{E2}	6.5	16.2	19.5	—	28.4	31.6	29.5	27.3	33.8	33.8	30.9

TABLE X: Average χ^2 and χ^2_{E2} over the number of nuclei fitted according to the results shown in Table IX.

	EXT	CQ	E(5)
$\overline{\chi^2}$	0.22	0.22	0.23
$\overline{\chi^2}_{E2}$	18.0	20.3	22.2